

A Study of Random Capacitor Networks to Assess the Emergent Properties of Dielectric Composites

P. RICHARDSON, D. P. ALMOND, AND C. R. BOWEN*

Materials Research Centre, Department of Mechanical Engineering, University of Bath, Bath, UK, BA2 7AY

This paper examines whether emergent behaviour is observed in dielectric composites, i.e. mixtures of two phases with zero conductivity and of permittivity ϵ_1 and ϵ_2 . The model developed enabled the study of random capacitor networks which contain capacitors of two different magnitudes (C_1 and C_2), which represent the two individual dielectric phases of a composite. The effective capacitance of the network was examined as a function of the individual capacitor magnitudes and their volume fraction. The capacitor networks exhibit an emergent region where there is low variability between individual random networks of a particular composition. The logarithm of the network capacitance scaled linearly with the logarithm of the capacitance ratio (C_1 and C_2), indicating that under particular conditions a logarithmic mixing rule can be used to determine the properties of dielectric mixtures.

Introduction

Significant interest remains in research related to the determination of the effective electrical properties of dielectric mixtures [1–9]. The type of mixtures considered range from synthetic composite materials with tailored electromagnetic properties, such as carbon-black epoxy [1] or polymer-ceramic nanocomposites [2], to natural composites such as wet rocks or ice [3]. Research has included experimental measurements [10], theoretical approaches [11] and computer simulations [4] and a number of reviews exist on the research which aims to correlate the permittivity of a heterogeneous mixture to the properties and distribution of its individual components [4–9].

Recent studies have demonstrated that the frequency dependent electrical characteristics of a two-phase conductor-insulator composite material are related to the intricate electrical network formed by the microstructure of the material [12, 13]. It was demonstrated that large networks of randomly positioned electrical components exhibit unexpectedly well-defined characteristics [14], described as ‘emergent scaling,’ whereby a logarithmic scaling rule [15] describes the conductance of the bulk network as a function of frequency. The study of mechanically loaded random networks [16] also revealed that these systems also have an emergent region, indicating that random networked systems may have a universal character.

The aim of this paper is to examine whether such emergent behaviour is observed in dielectric composites, i.e. mixtures of two phases of zero conductivity and of permittivity

Received August 26, 2008.

*Corresponding author. E-mail: c.r.bowen@bath.ac.uk

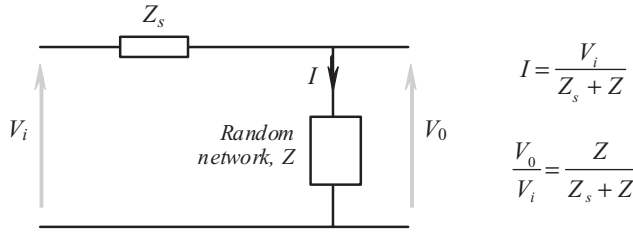


Figure 1. Initial model and model definitions.

ϵ_1 and ϵ_2 . The work examines the properties of random capacitor networks which contain capacitors of two different magnitudes (C_1 and C_2) which represent the two individual dielectric phases (ϵ_1 and ϵ_2) of a composite. The effective capacitance of the network (C_{eff}) is examined as a function of the individual capacitor values (C_1 and C_2) and volume fraction of each capacitor type (α).

Capacitor Network Development

Structure of the Model and Model Definitions. The model developed measured the impedance, Z , or admittance, Y , of a 2-dimensional random capacitor network. A voltage source V_i was applied to the network, as shown in Fig. 1, and the ratio of the voltage across the network to the current through the network provides the complex impedance. The series impedance, Z_s , in Fig. 1 represents the sum of the internal impedance of the voltage source and any additional series impedance which may be inserted into the circuit. A $100\text{k}\Omega$ series resistance was used in the model, which was sufficiently large to ensure a constant source current both over time and from one random network realisation to the next, yet was not so large as to render the total current impractically small.

The random network in Fig. 1 was built from a 2-dimensional rectangular array of ‘node points’. Impedances exist between a node and the nodes immediately above, below, left and right to form a grid of rectangular meshes as shown in Fig. 2. Each mesh was designated a 2-digit number where the first digit represents the mesh row and the second digit represents the mesh column (e.g. see ‘Mesh 24’ in Fig. 2). Mesh ‘00’ is an outer mesh in which the source and the series impedance of Fig. 1 reside. Row impedance $Z^r(m, n)$ is located on the top edge of Mesh mn while column impedance $Z^c(m, n)$ is located on the left-hand edge of Mesh mn . The impedance on the bottom edge of Mesh mn is therefore the impedance $Z^r(m + 1, n)$, providing m does not represent the bottom row, while that on the right-hand edge of Mesh mn is impedance $Z^c(m, n + 1)$, providing n does not represent the rightmost column. The impedances along the top and bottom rows are set equal to zero and these rows represent planar electrodes, as would be applied to a material when undertaking experimental capacitance measurements.

Determination of Currents Flowing Within the Model. Local currents flow around each mesh in the network and positive currents are defined such that the current I_{mn} flows clockwise around Mesh mn . From Kirchoff’s law, the sum of the voltages across each of the impedances around a mesh must equal the voltage sources in that mesh. As a result, these voltages must sum to zero. For example, for Mesh 24:

$$0 = Z_{24}^c(I_{23} - I_{24}) + Z_{24}^r(I_{14} - I_{24}) + Z_{25}^c(I_{25} - I_{24}) + Z_{34}^r(I_{34} - I_{24}) \quad (1)$$

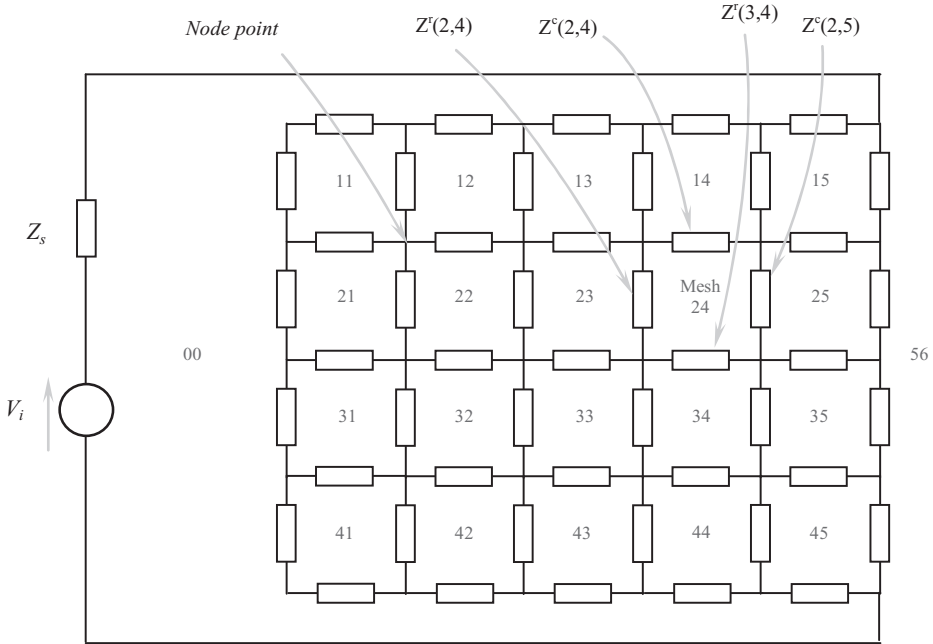


Figure 2. Image of rectangular two-dimensional grid showing node points and mesh.

or

$$0 = (-Z_{24}^c - Z_{24}^r - Z_{25}^c - Z_{34}^r)I_{24} + Z_{24}^c I_{23} + Z_{24}^r I_{14} + Z_{25}^c I_{25} + Z_{34}^r I_{34} \quad (2)$$

In the case of Mesh 00:

$$V = (Z + Z_{11}^c + \dots + Z_{41}^c + Z_{11}^r + \dots + Z_{15}^r + Z_{41}^r + \dots + Z_{45}^r)I_{00} - Z_{11}^c I_{11} - \dots - Z_{41}^c I_{41} - Z_{11}^r I_{11} - \dots - Z_{15}^r I_{15} - Z_{41}^r I_{41} - \dots - Z_{45}^r I_{45} \quad (3)$$

In the case of a Mesh 11 which borders Mesh 00 (Fig. 2):

$$0 = (-Z_{11}^c - Z_{11}^r - Z_{12}^c - Z_{21}^r)I_{11} + Z_{24}^c I_{00} + Z_{24}^r I_{00} + Z_{25}^c I_{12} + Z_{21}^r I_{21} \quad (4)$$

As a result of the impedances and the voltages V in Fig. 2 these equations represent $(4 \times 5) + 1$ simultaneous equations in $(4 \times 5) + 1$ unknown mesh currents and can be represented by the matrix below.

$$\begin{bmatrix} V \\ 0 \\ \vdots \\ 0 \end{bmatrix} = \underbrace{\begin{bmatrix} AA & AB & \dots & AZ \\ BA & BB & \dots & BZ \\ \vdots & \vdots & \ddots & \vdots \\ ZA & ZB & \dots & ZZ \end{bmatrix}}_{z \text{ - matrix}} \begin{bmatrix} I_{00} \\ I_{11} \\ \vdots \\ I_{45} \end{bmatrix} \quad (5)$$

The mesh currents within the network can be found by inverting the Z-matrix, such that,

$$\begin{bmatrix} I_{00} \\ I_{11} \\ \vdots \\ I_{45} \end{bmatrix} = \begin{bmatrix} AA & AB & \cdots & AZ \\ BA & BB & \cdots & BZ \\ \vdots & \vdots & \ddots & \vdots \\ ZA & ZB & \cdots & ZZ \end{bmatrix}^{-1} \begin{bmatrix} V \\ 0 \\ \vdots \\ 0 \end{bmatrix} \quad (6)$$

To solve the overall response of a $m \times n$ network, the Z-matrix elements can be solved by considering the mesh equations for Mesh mn :

$$\begin{aligned} 0 = & \underbrace{(-Z_{mn}^c - Z_{mn}^r - Z_{m(n+1)}^c - Z_{(m+1)n}^r)}_{\text{Column corresponding to mesh } mn \text{ (on the matrix diagonal)}} I_{mn} + \underbrace{Z_{mn}^c}_{\dots \text{to } m(n-1)} I_{m(n-1)} \\ & + \underbrace{Z_{mn}^r}_{\dots \text{to } (m-1)n} I_{(m-1)n} + \underbrace{Z_{m(n+1)}^c}_{\dots \text{to } m(n+1)} I_{m(n+1)} + \underbrace{Z_{(m+1)n}^r}_{\dots \text{to } (m+1)n} I_{(m+1)n} \end{aligned} \quad (7)$$

together with the equation for Mesh 00:

$$\begin{aligned} V = & \underbrace{(Z + Z_{11}^c + \cdots + Z_{N_r,1}^c + Z_{11}^r + \cdots + Z_{1N_c}^r + Z_{N_r,1}^r + \cdots + Z_{N_r,N_c}^r)}_{\text{Column corresponding to mesh 00 (on the matrix diagonal)}} I_{00} \\ & - \underbrace{Z_{11}^c}_{\dots \text{to } 11} I_{11} \cdots - \underbrace{Z_{N_r,1}^c}_{\dots \text{to } N_r,1} I_{N_r,1} - \underbrace{Z_{11}^r}_{\dots \text{to } 11} I_{11} \cdots - \underbrace{Z_{1N_c}^r}_{\dots \text{to } 1N_c} I_{1N_c} - \underbrace{Z_{N_r,1}^r}_{\dots \text{to } N_r,1} I_{N_r,1} \\ & - \cdots - \underbrace{Z_{N_r,N_c}^r}_{\dots \text{to } N_r,N_c} I_{N_r,N_c} \end{aligned} \quad (8)$$

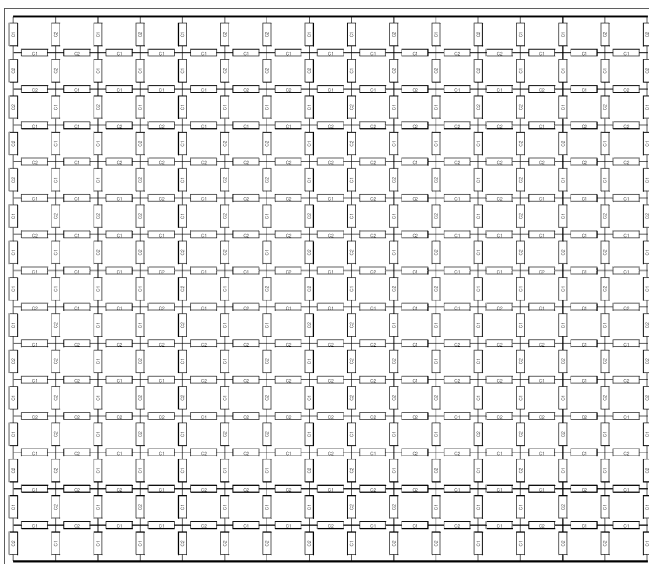
Now that a random network of electrical elements can be solved using the approach detailed above, the next stage is to construct random capacitor networks. To represent a dielectric composite consisting of two phases of different permittivity (ϵ_1 and ϵ_2) a network was built consisting of two individual capacitor types (C_1 and C_2). The fraction of each capacitor type C_1 and C_2 was defined as α_c and $(1 - \alpha_c)$ respectively.

Figure 3a shows a 16×16 random network and the upper and lower rows that form parallel-plate electrodes. Using a ‘dependent-probabilities’ method, there is exactly one component between each pair of nodes. To determine each component type, a random number was drawn from a uniform $U(0, 1)$ distribution. If the random number was below α_c , where $0 \leq \alpha_c \leq 1$, the component was capacitor C_1 . If the number was between α_c and unity, the component was a capacitor C_2 . The 16×16 random network shown in Fig. 3a has 15×16 column impedances and, on account of the parallel-plates, 14×15 operational row impedances. For an $n \times n$ network, this amounts to:

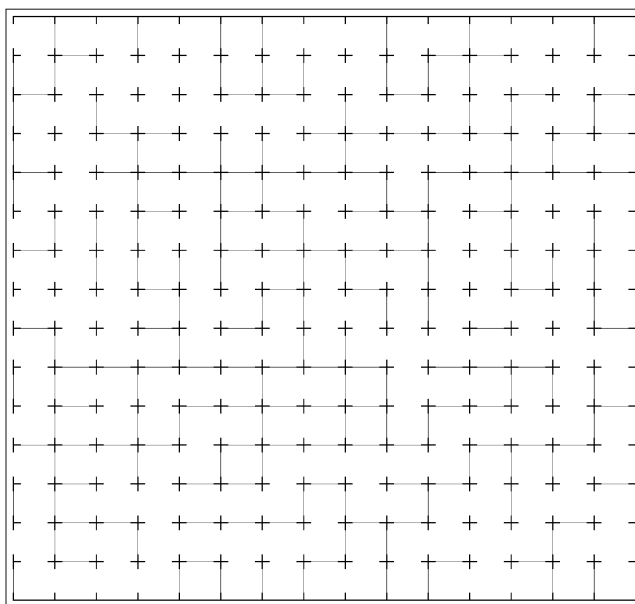
$$n(n-1) + (n-1)(n-2) = 2(n-1)^2 \quad (9)$$

impedances in total.

The complex ohmic values of the impedances found in this particular realisation of the network are given one of two imaginary (capacitive) values, corresponding to either C_1 or C_2 . Figure 3b and 3c show the location of capacitors C_1 and C_2 arise in a network where



(a)

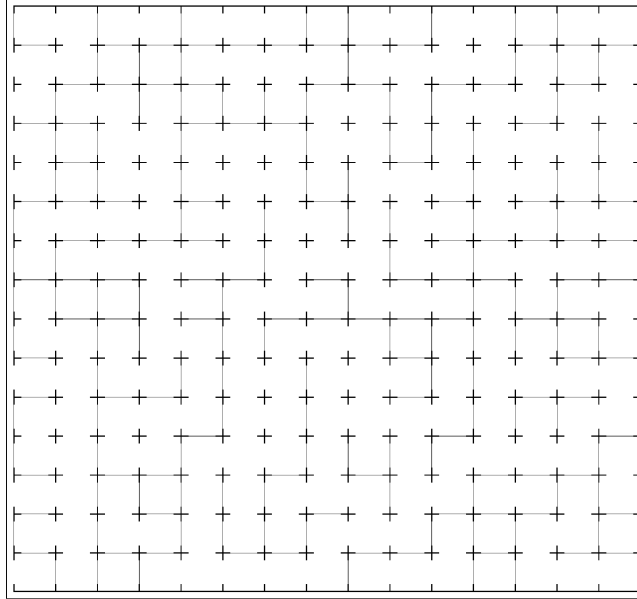


(b)

Figure 3. (a) A 16×16 random network with the upper and lower rows to form parallel-plate electrodes. There is one capacitor (C_1 or C_2) component between each pair of nodes. The location of capacitors C_1 (b) and C_2 (c) in a network are shown for $\alpha_c = 0.5$.

$\alpha_c = 0.5$ (i.e. a 50:50 mixture of C_1 and C_2). Each node is filled with a capacitor in either one or the other of the figures (Fig. 3b–c).

Capacitor Values Used in the Random Network Model. This final section provides details of the electrical conditions used in the network. The ratio of the susceptances of the C_1 and



(c)

Figure 3. (Continued)

C_2 capacitors is given by,

$$j\omega C_1 : j\omega C_2 \tag{10}$$

In order to provide a large range of contrasting C_1 and C_2 magnitudes for the capacitors in an attempt to model dielectric mixtures containing phases of different permittivity, the model sets ω and C_2 as constants and C_1 was gradually increased from very small values to very large values (i.e. from $C_1 \ll C_2$ to $C_1 \gg C_2$). It is assumed $C_1 = k\bar{C}_1$ where \bar{C}_1 is a constant. The ratio of the two susceptances is then:

$$jk\bar{C}_1 : j\omega C_2 \tag{11}$$

$$jkB_1 : jB_2 \tag{12}$$

where $B_1 = \omega\bar{C}_1$ and $B_2 = \omega C_2$ are both constant susceptance terms. In the model, k ranges from 200 to 2×10^9 and by setting $\bar{C}_1 = 10^{-14}$ (i.e. 0.01 pF), $C_1 = k\bar{C}_1$ varies between 2 pF and 20 μ F. The value of C_2 was fixed at a constant magnitude between the two extremes of values for C_1 so that the ratio C_1/C_2 (defined as ‘contrast’) varied from small (~ 0.0001) to large values (~ 100000). The model was solved at each increment of C_1 . The angular frequency, ω , is fixed at 10 M rad s^{-1} , corresponding to a frequency of 1.59 MHz, so that $B_1 = \omega\bar{C}_1 = 10$ nS and $B_2 = \omega C_2 = 1$ mS.

Results

Networks were modelled with different C_1 and C_2 volume fractions ($\alpha_c = 0.3, 0.5$ and 0.7) and multiple random networks were examined at the same fraction to study the variability

of the network capacitance as a result of different random arrangements of C_1 and C_2 . The model output results for 30 realisations of the random network with a 50:50 ratio of capacitors C_1 and C_2 (i.e. $\alpha_c = 0.5$) are shown in Fig. 4a. Network results for a 30:70 and 70:30 ratio of capacitors C_1 and C_2 (i.e. $\alpha_c = 0.3$ and 0.7) are shown in Fig. 4b and Fig. 4c respectively.

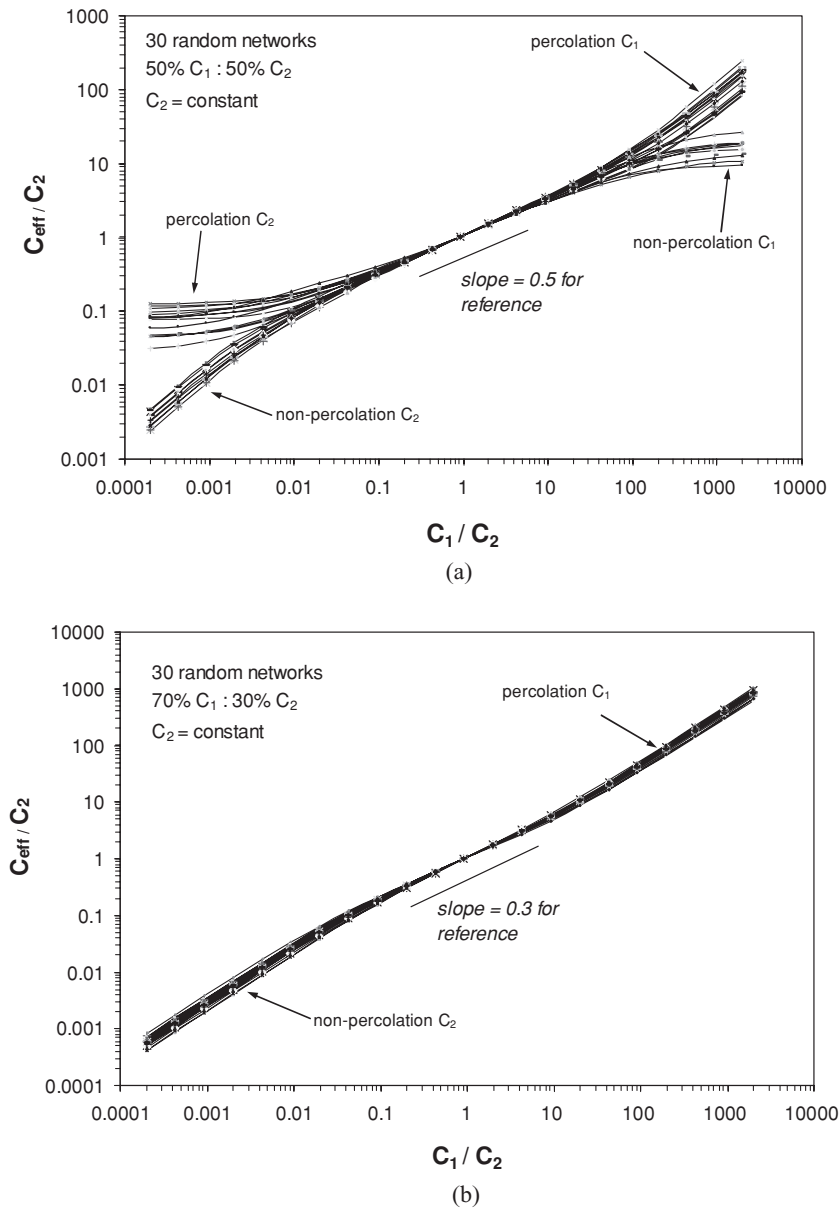


Figure 4. Network results of 30 individual random networks consisting of capacitors of values C_1 and C_2 of composition (a) $\alpha_c = 0.5$ (50:50 mix), (b) $\alpha_c = 0.7$ (70:30 mix) (c) $\alpha_c = 0.3$ (30:70 mix).

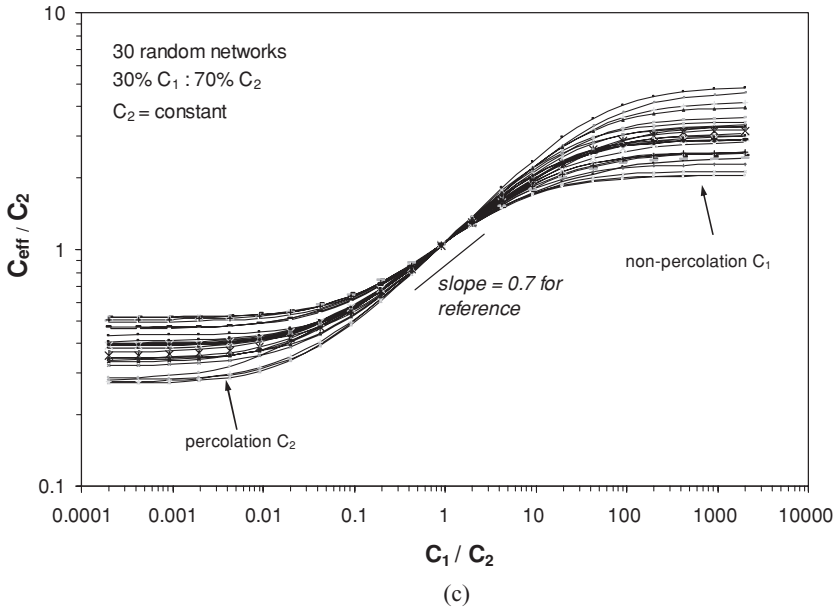


Figure 4. (Continued)

Similar observations can be made to the results for frequency dependent properties of resistor-capacitor networks [12] and mechanical networks [16]. The capacitor networks exhibit emergence in the central region of the graphs in Fig. 4a–c where there is low variability between individual random networks of a particular composition (see for example Fig. 4a). In this region the contrast (C_1/C_2) between the values of the two capacitor values is relatively low and currents are likely to be flowing through both capacitor types. Figure 5 shows the variability (bandwidth) of networks as function of capacitor contrast (C_1/C_2) for each network composition.

In the region of low variability (emergent region) a logarithmic scaling rule describes the capacitance of the network,

$$C_{eff} = C_1^{\alpha_c} \cdot C_2^{1-\alpha_c} \tag{13}$$

Rearranging Equation 13 gives rise to,

$$\frac{C_{eff}}{C_2} = \left(\frac{C_1}{C_2} \right)^{\alpha_c} \tag{14}$$

Equation 14 indicates that the gradient of $\log(C_{eff}/C_2)$ versus $\log(C_1/C_2)$ data, as plotted in Fig. 4, should equal the fraction of C_1 capacitors (α_c). Figures 4a–c indicates that very good agreement exists between the slope of the central emergent region and the volume fraction of C_1 , as also observed by Murphy et al. [16] for mechanical networks. The extent (width) of the emergent region has also been observed to increase with network size [16].

At the extremes of capacitor contrast (high or low C_1/C_2) the variability between the networks increases (see Fig. 4 and Fig. 5) and no emergent region exists. At high contrast values the degree of connectivity of the capacitors is important due to percolation paths of connected C_1 or C_2 capacitors. For example if $C_1 \gg C_2$ (high C_1/C_2) currents will

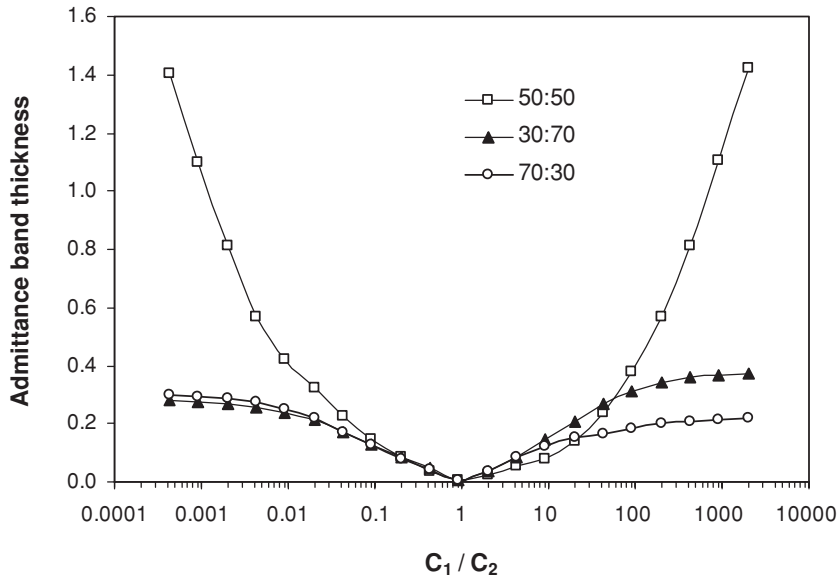


Figure 5. Variability of networks as function of capacitor contrast (C_1/C_2) for each network composition.

preferentially flow through C_1 at a specific frequency due to its higher susceptance. For the network with a 70:30 ratio of C_1 and C_2 (i.e. $\alpha_c = 0.7$) the C_1 are in a majority and are likely to percolate across the network, while C_2 is in the minority and is unlikely to percolate through the network. In this case when $C_1 \rightarrow 0$ and $C_1 \ll C_2$ (left hand side of Fig. 4b) the 70:30 network value approaches very small values and when $C_1 \gg C_2$ and $C_1 \rightarrow \infty$ the network approaches very large values (right hand side of Fig. 4b). However, for a 30:70 ratio of C_1 and C_2 capacitors (i.e. $\alpha_c = 0.3$) the C_1 components are in a minority and are unlikely to percolate across the network, while C_2 is in the majority and is likely to percolate across the network. As a result, when $C_1 \ll C_2$ the C_1 acts like an open circuit and the network value approaches a constant value (left hand side Fig. 4c). Similarly when $C_1 \gg C_2$ the C_1 acts like a closed circuit and the network value approaches a constant, but higher, value (right hand side in Fig. 4c). For a 50:50 mixture of C_1 and C_2 (Fig. 4a) percolation of C_1 and/or C_2 is possible giving rise to all four potential conditions at high levels of capacitor contrast (left and right hand sides of Fig. 4a).

Conclusions

This work has examined the properties of networks of random capacitors in an attempt to model the behaviour of dielectric composites. The capacitor networks exhibit an emergent region where there is low variability between individual random networks of a particular composition. For high capacitor contrast (i.e. $C_1 \ll C_2$ or $C_1 \gg C_2$) the overall capacitance of the networks of the same composition was observed to be highly variable (Fig. 5) and strongly dependent on the degree of connectivity and the presence of percolation paths within the networks (Figs. 4a–c).

While the degree of ‘connectivity’ [17] of the two phases is often considered to be important, the observed emergent behaviour demonstrates that for composites containing

dielectric phases with low contrast (i.e. relatively low difference between ε_1 and ε_2) a simple logarithmic mixing rule [15] can be used to predict the composite dielectric constant (ε_{eff}), namely:

$$\varepsilon_{eff} = \varepsilon_1^\alpha \cdot \varepsilon_2^{1-\alpha} \quad (15)$$

where α is the volume fraction of phase ε_1 .

This work is of relevance when the effective dielectric constant of the composite must be known based on mixtures two (or more) phases of different dielectric constant. The networks developed are also of interest in studying the variation in properties of dielectric composites or designing composites with low variability.

References

1. K. C. Cheng, C. M. Lin, S. F. Wang, S. T. Lin, and C. F. Yang, Dielectric properties of epoxy resin–barium titanate composites at high frequency. *Mat. Lett.* **61**, 757–760 (2007).
2. Y. Rao, J. Qu, T. Marinis, and C. P. Wong, A precise numerical prediction of effective dielectric constant for polymer–ceramic composite based on effective-medium theory. *IEEE Trans. Compon. Pack. Tech.* **23**, 680–683 (2003).
3. A. H. Sihvola, Effective permittivity of dielectric mixtures. *IEEE Trans. Geosci. Rem. Sens.* **26**, 420–429 (1988).
4. Y. Wu, X. Zhao, F. Li, and Z. Fanj, Evaluation of mixing rules for dielectric constants of composite dielectrics by MC-FEM calculation on 3D cubic lattice. *J. Electroceram.* **11**, 227–239 (2003).
5. K. Lal and R. Parshad, The permittivity of heterogeneous mixtures. *J. Phys. D: Appl. Phys.* **6**, 1363–1368 (1973).
6. B. Sareni, L. Krähenbühl, and A. Beroual, Effective dielectric constant of random composite materials. *J. Appl. Phys.* **81**, 2375–2385 (1997).
7. E. Tuncer, Y. V. Serdyuk, and S. M. Gubanski, Dielectric mixtures: Electrical properties and modelling. *IEEE Trans. Dielect. Elec. Ins.* **9**, 809–828 (2002).
8. J. A. Reynolds and J. M. Hough, Formulae for dielectric constant of mixtures. *Proc. Phys. Soc. B* **70**, 769–775 (1957).
9. L. S. Taylor, Dielectric properties of mixtures. *IEEE Trans. Ant. Prop.* **13**, 943–947 (1965).
10. M. E. Achour, M. El. Malhi, J. L. Miane, F. Carmona, and F. Lahjomri, Microwave properties of carbon black–epoxy resin composites and their simulation by means of mixture laws. *J. App. Pol. Sci.* **73**, 969–973 (1999).
11. A. H. Sihvola, How strict are theoretical bounds for dielectric properties of mixtures? *IEEE Trans. Geosci. Rem. Sens.* **40**, 880–886 (2002).
12. D. P. Almond and B. Vainas, The dielectric properties of random R–C networks as an explanation of the ‘universal’ power law dielectric response of solids. *J. Phys.: Cond. Matt.* **11**, 9081–9093 (1999).
13. D. P. Almond, C. R. Bowen, and D. A. S. Rees, Composite dielectrics and conductors: simulation, characterisation and design. *J. Phys. D: Appl. Phys.* **39**, 1295–1304 (2006).
14. R. Bouamrane and D. P. Almond, The ‘emergent scaling’ phenomenon and the dielectric properties of random resistor-capacitor networks. *J Phys.: Cond. Matt.* **15**, 4089–4100 (2003).
15. K. Lichtenecker and K. Rother, Die Herleitung des logarithmischen Mischungs-gesetzes aus allgemeinen Prinzipien der stationären Stromung. *Physik. Zeitschr.* **32**, 255–260 (1931).
16. K. D. Murphy, G. W. Hunt, and D. P. Almond, Evidence of emergent scaling in mechanical systems. *Phil. Mag.* **86**, 3325–3338 (2006).
17. R. E. Newnham, D. P. Skinner, and L. E. Cross, Connectivity and piezoelectric-pyroelectric composites. *Mat. Res. Bull.* **13**, 525–536 (1978).